# Quasicontinuum relativistic many-body perturbation theory photoionization cross sections of Na, K, Rb, and Cs

I. M. Savukov*
*Los Alamos National Laboratory, Los Alamos, New Mexico 87545, USA*
(Received 8 August 2007; published 17 September 2007)

Calculations of photoionization cross sections for alkali-metal atoms are carried out in the framework of relativistic many-body perturbation theory (RMBPT) using quasicontinuum *B*-spline orbitals. All third-order terms are included, in contrast to previous calculations based on either random-phase approximation (RPA), Brueckner orbitals, or their combination. The particular advantage of quasicontinuum states is that high-order MBPT codes do not require modification for applications to the photoionization problem. The agreement with experiment is improved compared to RPA and Dirac-Hartree-Fock approximations. The results also exhibit close form invariance. The presented formalism can be extended to other photoionizing transitions.

DOI: 10.1103/PhysRevA.76.032710 PACS number(s): 32.80.Fb, 31.10.+z, 31.15.Ar, 31.30.Jv

## I. INTRODUCTION

Photoionization cross sections are important in many applications such as astrophysics, plasma physics, atmospheric science, and lighting industry. Despite a long history of their measurements and calculations, current availability of high-quality synchrotron radiation sources in vacuum-ultraviolet and x-ray spectra, and impressive progress in precision of atomic theory for bound state properties, the photoionization cross sections for most atoms remain mostly uncertain. It is particularly intriguing in the case of alkali-metal (AM) atoms, which can be regarded among the simplest atoms for theory. For example, otherwise highly accurate relativistic many-body perturbation theory (RMBPT) methods when applied to bound-bound transition reach much lower accuracy for alkali-metal atoms in calculations of photoionization cross sections, which are essentially proportional to squares of dipole matrix elements (MEs) between bound and continuum states. So why are the bound-bound MEs much more accurate than the bound continuum?

From the analysis of experimental techniques employed for measurements of photoionization cross sections of AM atoms, it appears that the accuracy of experimental data was limited by uncertainty in the density calibration and systematic effects due to AM molecules. The AM molecules were particularly problematic since they were always present along with AM atoms and their cross sections were not known well. Marr and Creek [1] observed molecular absorption in the vicinity of the atomic ionization threshold and used different temperature measurement to exclude the effects of molecules. Photoionization cross sections of Rb, $Rb_2$, Cs, and $Cs_2$ were measured in Ref. [2] and were used along with other available data, including absolute cross section of Ref. [3] in which the density was measured directly with a hot-wire ionizer, to reanalyze Rb and Cs photoionization cross sections. It seems that the best experimental value for Cs at the threshold energy is 0.1 Mb, which differs 2 times from the older measurement of Marr and Creek [1], 0.2 Mb, with the uncertainty in density being responsible for such large disagreement. In the case of Rb, normalization in Ref. [2] has been done on semiempirical values of Ref. [4], which can introduce systematic errors, despite the ability of theory to follow relative experimental cross sections. Significant uncertainty is also present in other AM atoms.

Accuracy of theory, on the other hand, strongly depends on the type of the atom and the energy range and can be quite low. Within the AM sequence, the Li atom can be calculated with the highest precision, which is obvious from the comparison of Dirac-Hartree-Fock (DHF) and relativistic random-phase approximation (RRPA) theories that reveal smallness of correlation corrections, but the precision for other AM atoms as judged by such comparison is progressively lower from Na to Cs (see, e.g., Ref. [5]). The difficulties for theories are primary due to correlation corrections, strong cancellation in lowest order, especially near cross section zeros, and to some degree relativistic corrections. Most atoms have significant polarizabilities and including many-body effects beyond DHF approximation is essential. This can be done consistently in the framework of RMBPT, which is the subject of this work. Previously RMBPT calculations were performed at the level of RRPA and Brueckner-orbital (BO) approximation [5,6]. Relativistic effects are also important: fine-structure continuum components have considerably different contributions to the photoionization cross sections than expected from nonrelativistic theory. Even though photoionization theories might have accuracy issues, they are still very important not only for the understanding of experimental observations and exclusion of systematic errors in measurements, but also for extending the photoionization database to include more transitions and to increase energy range.

In order to achieve confidence in theoretical values, comparison with experiment is essential for benchmark systems as well as good understanding of atomic interactions in such systems. This is why it is important to systematically study alkali-metal atoms, especially on the subject of many-body effects involving continuum states, which are still not well understood compared to the level of understanding achieved for transitions of bound states.

In this paper, the method of quasicontinuum states will be used to allow the application of accurate transition (third and

*isavukov@lanl.edu

 

higher order) and energy (second and higher order) RMBPT codes without modifications to calculations of photoionization cross sections of Na, K, Rb, and Cs. This is the extension of quasicontinuum RMBPT theory previously applied to the calculations of electron elastic scattering cross sections on noble-gas atoms [7]. The form-invariant (FI) third-order RMBPT and its modified versions that include some diagrams in high (infinite) order will be illustrated. In the third order, the MBPT contains a large number of nontrivial diagrams, so it is indeed of clear advantage to be able to use *no-modification* approach. Furthermore, for other atoms, calculations based on configuration-interaction RMBPT can be performed in the future, as the extension of the approach presented here.

Previously, some subsets of third-order diagrams were used [6], but neglecting others is not much justified. It is possible that, for example, structural radiation (SR) corrections neglected in previous calculations are large. Another important point is that BO-chain corrections, also not considered in previous calculations, can have significant contributions to the phase of a continuum wave function, as was shown in Ref. [7] where BO diagonalization was essential to obtain agreement with experiment for phase shifts and cross sections. Some uncertainty in the method proposed here might have existed due to the extraction of a coefficient of proportionality between quasicontinuum and continuum wave functions obtained from a quasicontinuum spectrum according to the method of Ref. [8], but the agreement of our results based on cavity calculations in DHF and RRPA approximations with DHF and RRPA results based on continuum wave functions [5,9] gives assurance in the accuracy of the normalization in the quasicontinuum approach.

## II. THEORY

### A. Photoionization cross-section formula for quasicontinuum states

Photoionization cross sections are similar to absorption cross sections of transitions between discrete states, both being related to electric-dipole matrix elements (MEs). The main difference is in normalization. Disregarding small differences in normalization between relativistic and nonrelativistic wave functions of low-energy electrons, we can use the nonrelativistic solution of the normalization problem developed in Ref. [8]. According to Ref. [8], the ratio between a nonrelativistic quasicontinuum radial wave function $P_{nl}(r)$, where $n$ is the principal and $l$ is the orbital quantum number, and a continuum wave function $P_{\epsilon_l}$, where $\epsilon$ is the electron energy, can be found from quasicontinuum energies $E_{nl}$,

$$\left(\frac{P_{\epsilon_l}}{P_{nl}}\right)^2 = \frac{1}{\partial E_{nl}/\partial n} \approx \frac{2}{E_{n+1l} - E_{n-1l}}. \tag{1}$$

The relation between continuum and quasicontinuum wave functions is also intuitively obvious from considering Thomas-Reiche-Kuhn (TDK) sum rule for the oscillator strengths $f$,

$$\sum_n f_n + \int_0^\infty \frac{df}{d\epsilon} d\epsilon = N \tag{2}$$

($N$ is the number of electrons in an atom, $\epsilon$ is the photoelectron energy, $n$ runs over discrete states), in which the integration over continuum can be replaced by the summation over discrete quasicontinuum states to obtain the same result with high precision.

The photoionization cross section can be calculated using a simple expression given in Ref. [10],

$$\sigma(E) = 4.03 \times 10^{-18} \frac{df}{d\epsilon}\ \mathrm{cm}^2, \tag{3}$$

where $E$ is the photon energy. The energy derivative of photoionization oscillator strength $f$ for photoelectron energy $E_{nl}$ can be calculated by dividing the oscillator strength $f(E_{nl})$ for the transition to a quasidiscrete state $nl$ by an energy interval with an adjacent state (upper or lower), or in symmetric version, more accurately, by a half-interval between the upper and lower adjacent states as in Eq. (1),

$$\frac{df}{d\epsilon} \approx \frac{2f(E_{nl})}{(E_{n+1l} - E_{n-1l})}. \tag{4}$$

If relativistic calculations are performed, the cross sections due to $p_{1/2}$ and $p_{3/2}$ states should be added to obtain total photoionization cross section from the ground state.

The advantage of the approach based on quasicontinuum instead of continuum states is the possibility to use accurate and complicated high-order (R)MBPT codes developed for discrete states without any modification. However, the above equation introduces some error due to its approximate nature, and comparison with calculations based on continuum states is needed to estimate this error.

### B. RMBPT

Third-order FI RMPBT theory for transition amplitudes to be applied here is described in Ref. [11] and references therein. The RMBPT expansion is performed in the "frozen" $V^{(N-1)}$ DHF Hamiltonian basis which is most convenient for one-valence electron atoms and ions because many *potential* diagrams that exist in alternative bases vanish. This basis also automatically incorporates dominant relativistic effects, in particular the spin-orbit interaction. Because the $V^{(N-1)}$ DHF basis contains continuum states as well as an infinite number of Rydberg states, it is inconvenient in practical calculations. Instead a compact discrete $B$-spline basis of $V^{(N-1)}$ DHF Hamiltonian in a cavity that approximates accurately lowest bound states and replaces continuum and Rydberg states with a finite number of discrete states is introduced. Technically this cavity-bound basis is constructed by solving the DHF equation in a small $B$-spline basis, and the resulting DHF cavity-bound basis functions are approximated by the linear combinations of $B$ splines that are eigensolutions of the DHF Hamiltonian matrix. To check numerical accuracy of results, the calculations for several cavity sizes and number of splines were performed. It turned out that the 40-spline basis was much less accurate than that of 60 splines,

so the latter was chosen for final calculations. The consequence of insufficiency of the number of splines was exhibited in dramatic increase of intervals between quasicontinuum states and in "disappearance" of expected quasicontinuum states.

The "bag" boundary condition is imposed $P(R)=Q(R)$ instead of nonrelativistic $P(R)=0$ [and presumably $Q(R)=0$], where $R$ is the cavity radius and $P$ and $Q$ are large and small components, to avoid spurious solutions from negative-energy continuum. The "bag" boundary condition is closely equivalent to a nonrelativistic one as far as normalization is concerned if the velocity of the electron near the boundary is much slower than the speed of light. For low-energy photoionization this condition is well satisfied and the theory laid out in the preceding section for the nonrelativistic boundary condition immediately applies to relativistic calculations.

The summation over magnetic sublevels in RMBPT expression is performed analytically with the aid of the Wigner-Eckart theorem and angular momentum diagrams (see, e.g., Ref. [12]) to increase computational speed. Since it is well known that in general results in the length and velocity forms can be substantially different, matrix elements and cross sections in both forms are calculated and compared.

### C. Brueckner orbitals

As shown in Ref. [7], all-order Brueckner orbital (BO) corrections can be important to achieve good accuracy of phase shifts of continuum wave functions, so in this paper in addition to the third FI theory, we apply a complete third order theory that also incorporates all-order BO corrections. The Brueckner orbitals for this theory are calculated in a cavity DHF $B$-spline basis as the eigenvectors of the Hamiltonian matrix $H_{ij}^{\mathrm{BO}}$,

$$H_{ij}^{\mathrm{BO}} = \delta_{ij}\epsilon_j + \Sigma_{ij}(\varepsilon_0), \tag{5}$$

where the self-energy matrix $\Sigma_{ij}$,

$$\Sigma_{ij}(\varepsilon_0) = \sum_{kcmn} \frac{(-1)^{j_m+j_n-j_i-j_c}}{(2j_i+1)(2k+1)} \frac{X_k(icmn)Z_k(mnjc)}{\varepsilon_0+\varepsilon_c-\varepsilon_m-\varepsilon_n} + \sum_{kbcn} \frac{(-1)^{j_i+j_n-j_b-j_c}}{(2j_i+1)(2k+1)} \frac{X_k(inbc)Z_k(bcjn)}{\varepsilon_0+\varepsilon_n-\varepsilon_b-\varepsilon_c} \tag{6}$$

is obtained from a second-order RMBPT energy by replacing two of the same initial and final valence states $v$ with two arbitrary states $i$ and $j$ and the DHF energy of the valence state $\varepsilon_v$ with a fixed energy $\varepsilon_0$, the same for a set of BOs of a given angular momentum. (Notations are the same as in Ref. [7].) Because the dependence of BOs on $\varepsilon_0$ is relatively slow, for convenience we choose the zero-order DHF energy $\varepsilon_v$ as $\varepsilon_0$ instead of more accurate higher-order energies. However, it would be inappropriate to use energies that are different by more than 0.1 a.u., which might be attractive because it would save computation time if we could use, for example, $9p$ energy for calculating $9p$ and $10p$ quasicontinuum BOs. One indication of the problem is substantial decrease in form invariance of results if wrong energies are used. Brueckner orbitals based on the DHF basis contain automatically dominant relativistic corrections. Because the $B$-spline basis in the cavity is discrete, the diagonalization of the BO Hamiltonian is straightforward.

The all-order BO energy rather than the second-order RMPBT energy $E_v^{(2)}=\Sigma_{vv}(\varepsilon_v)$ was important for obtaining correct phase shift of continuum wave functions in Ref. [7] because higher-order "chain" BO terms are not small due to smallness of denominators $(\epsilon_v-\epsilon_i)$,

$$E_v^{(4)} + E_v^{(6)} + \cdots = \sum_{i\neq v} \frac{\Sigma_{vi}(\varepsilon_0)\Sigma_{iv}(\varepsilon_0)}{\varepsilon_v-\varepsilon_i} + \sum_{i\neq v, j\neq v} \frac{\Sigma_{vi}(\varepsilon_0)\Sigma_{ij}(\varepsilon_0)\Sigma_{jv}(\varepsilon_0)}{(\varepsilon_v-\varepsilon_i)(\varepsilon_v-\varepsilon_j)} + \cdots. \tag{7}$$

Moreover, in the case of true continuum states the denominators can be infinitely small, leading to an apparent convergence problem. Thus quasicontinuum states are more convenient than true continuum states in RMBPT for these particular diagrams where vanishing denominators can be encountered, although we do not need to calculate these diagrams separately because the diagonalization of the BO Hamiltonian $H_{ij}^{\mathrm{BO}}$ produces accurate BO energies that automatically include all "chain" self-energy corrections $E_v^{(4)}$, $E_v^{(6)}$, etc. It is also worth mentioning that the high-order terms that are not derivatives of the BO chain are expected to be less important for phase shifts of low-energy continuum states because the denominators in these terms are not small, being on the order of core-excitation energy. This is true as long as quasicontinuum energy does not approach the core-excitation energy (on the order of 1 a.u.). In the case when it does approach the core-excitation energy, small denominators can appear in many diagrams and the perturbation theory will be inaccurate. Thus the energy range above 0.5 a.u. is avoided in current calculations.

The third-order BO $Z_{\mathrm{BO}}^{(3)}$ and BO chain corrections for transition MEs such as $Z_{\mathrm{BO}}^{(5)}$ and of higher orders

$$Z_{vw}^{\mathrm{BO}} = Z_{\mathrm{BO}}^{(3)} + Z_{\mathrm{BO}}^{(5)} + \cdots = \sum_{i\neq v} \frac{\Sigma_{vi}(\varepsilon_0)Z_{iw}}{\epsilon_v-\epsilon_i} + \sum_{i\neq w} \frac{Z_{vi}\Sigma_{iw}(\varepsilon_0)}{\epsilon_w-\epsilon_i} + \sum_{i,j\neq w} \frac{Z_{vi}\Sigma_{ij}(\varepsilon_0)\Sigma_{jw}(\varepsilon_0)}{(\epsilon_w-\epsilon_i)(\epsilon_w-\epsilon_j)} + \cdots \tag{8}$$

also play an important role due to the same reason of smallness of denominators $\epsilon_w-\epsilon_i$ and $\epsilon_w-\epsilon_j$ when $w$, $i$, and $j$ are quasicontinuum states and the cavity is large. Moreover, these denominators become infinitely small in the case of continuum. It is interesting to note that there is enhanced sensitivity of MEs to the phase shifts of continuum wave functions at energy at which due to oscillatory nature of these wave functions cancellation can occur. Because the inclusion of BO chain corrections dramatically affected phase shifts, it is anticipated that these corrections can be significant in calculations of bound-continuum transitions. In order to include this important effect we will use the BO basis obtained by diagonalization of the Hamiltonian matrix defined by Eq. (5).

As alternative to the approach described here, BOs can be also obtained by solving the differential equation which includes nonlocal correlation potential $\Sigma(\mathbf{r},\mathbf{r}')$ [13,14]. Thus the problems of small denominators in chain diagrams and infinite dimension for a continuum basis are avoided.

### D. RRPA matrix elements

It is well known that RPA (relativistic version, RRPA) corrections are large and if included bring cross sections calculated in length and velocity forms in agreement (Ref. [5] and references therein). In the current theory, RRPA corrections are included following the procedure described in Ref. [11] at the level of third-order form-invariant theory. While in second-order theory there is only a RPA ME between initial and final valence states $Z_{vw}^{\mathrm{RPA}}$, in the expressions of third FI MBPT, there are also MEs between arbitrary states, $Z_{ij}^{\mathrm{RPA}}$, which inclusion was necessary for obtaining precise agreement of AM transition amplitudes calculated in length and velocity forms. One parameter relevant to calculations described in Ref. [11] is the number of core-RPA iterations. In the current calculations, it is chosen 20, which saturates well convergence and is sufficient to achieve a high level of agreement between length and velocity forms.

### E. Third-order FI theory and BO+SR+RPA theory

In Ref. [11], high-accuracy third-order FI theory (FI3) has been developed and applied to alkali-metal resonant transitions. A point of deviation from conventional third-order theory described in Ref. [15] is that in the FI theory DHF MEs are replaced with RPA MEs and derivative terms are added. The application of the FI3 theory to photoionization in current work goes well beyond previous attempts of including MBPT terms at relatively simple levels such as RPA (Ref. [5] and references therein), third-order BO, or their combination [6]. The current theory includes not only all third-order corrections but also some diagrams such as RPA, which are very important for photoionization, in high order (iterated 20 times the core-RPA diagram). From the analysis of results in this work it is found that even complete FI third-order theory is not sufficient in heavy atoms because it does not contain substantial high-order (beyond third) BO corrections. So previous FI3 theory is modified to include all-order BO corrections. This is done by implementing third-order calculations in the BO basis obtained by diagonalization of the BO Hamiltonian matrix built in the quasicontinuum DHF $B$-spline basis. The BO basis has energies correct to second order and is automatically normalized, so the derivative and normalization terms as well as the third-order BO term (to avoid double counting) are excluded. Structure-radiation (SR) as well as RPA terms, on the other hand, are retained. This, the most complete theory of photoionization of AM atoms, will be referred to as the BO+SR+RPA theory. Previously, similar theory that includes BO, RPA, SR corrections was successfully applied to calculations of various low-state discrete Cs transitions [16].

### F. Form independence and numerical accuracy

Form independence of results calculated using form-independent theories is a good cross check of numerical accuracy and various errors. Form independence of present photoionization RRPA cross sections based on 60 splines was in the case of Na at the level of four digits, but went down to 1% level in the case of Cs, which can be attributed to the reduction in accuracy of $B$-spline approximation, incompleteness of the basis, and the smallness of RRPA MEs due to cancellations. On the other hand, 1% level form independence of results at low energy with the same basis was achieved in calculations with the FI3 theory for both Na and Cs. This level of form independence provides important verification of sufficient numerical accuracy. In addition, we discovered that the BO+SR+RPA results were also fairly form independent. In the Cs case at low energy, length-velocity difference was on the order of 7%, and in the Na case about 2%. This agreement not only provides confidence in numerical accuracy and absence of crude mistakes for calculations with a new code (the BO+RPA+SR code is obtained by modification of the extensively tested FI3 code), but also removes uncertainty with respect to the choice of the form of the transition operator. Very often the accuracy of calculations is estimated from the length-velocity variation, which in the case of FI theories would not be appropriate, but in the case of form-dependent theory such as BO+RPA+SR can be used. The form agreement gives also the confidence in the accuracy of the BO basis consisting of only 20 excited states.

## III. PHOTOIONIZATION CROSS-SECTION CALCULATIONS AND COMPARISON OF RESULTS

In this section, the results of calculations using quasicontinuum $B$-spline wave functions will be presented for Na, K, Rb, and Cs and compared with other calculations and measurements. Because experiments have significant uncertainties, comparison for several AM atoms is important to judge the accuracy of theory. Different approximations such as DHF, RRPA, BO, third-order FI RMPT, and BO+RPA+SR are compared to illustrate the significance of correlation corrections.

### A. Na photoionization cross section

To evaluate the accuracy of normalization, which might contain uncertainty due to use of quasicontinuum wave functions, in Fig. 1 we compare current quasicontinuum DHF length-form cross sections with the length-form DHF cross sections calculated using conventional continuum wave functions in Ref. [9]. The current 60-spline quasicontinuum calculations are in close agreement with the results of Ref. [9]. Next in Fig. 2 we show a comparison of calculations in various MBPT approximations with experiment. First, our most accurate values, third-order MBPT (40 and 60 spline) and BO+RPA+SR (60 splines) closely agree and are quite accurately form independent. Our RRPA results (60 splines) deviate substantially from RRPA results of Ref. [5] at low momentum, but agree quite accurately for $p>0.25$ a.u. Although the normalization problem might have been present in the current quasicontinuum calculations, close agreement of DHF values in the current work with those of Ref. [9] indicates that normalization in the current calculations is

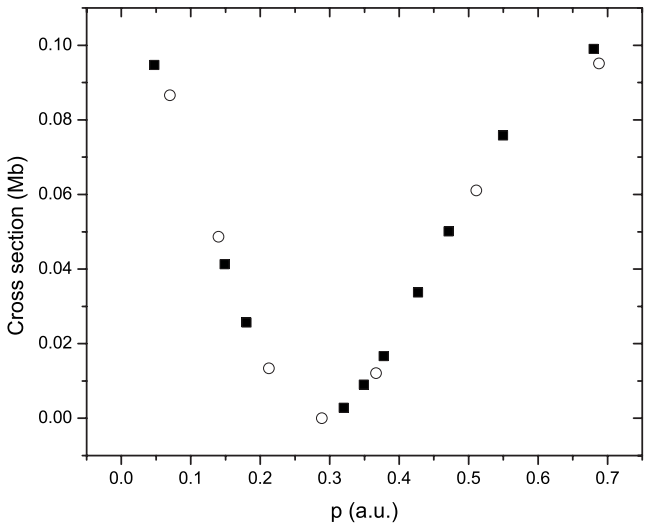


FIG. 1. Comparison of Na DHF length-form photoionization cross sections: squares, results of Ref. [9]; open circles, current 60-spline quasicontinuum calculations.

quite accurate. There is good agreement of our RRPA cross section (for example, at $p=0.1$ $\sigma=3.15\times10^{-20}$ cm$^2$) with the RRPA cross section of Ref. [17], $\sigma=3.583\times10^{-20}$ cm$^2$ at $p=0.1$, while the RRPA result of Ref. [5] is $\sigma=5.14\times10^{-20}$ cm$^2$, suggesting that our RRPA values at low momentum are more accurate than those of Ref. [5]. At $p=0.5$ and $p=0.7$, the three calculations agree precisely. In other alkali-metal atoms (following sections), our quasicontinuum RRPA results agree closely with those of Ref. [5], so the disagreement for Na at low momentum is quite anomalous.

The third order calculations definitely improve the agreement with experiment compared to RRPA. However, even the most precise calculations have some disagreement with experiment. The disagreement can be partially attributed to experimental problems such as uncertainty of contributions of AM diatomic molecules and uncertainty in AM density, as

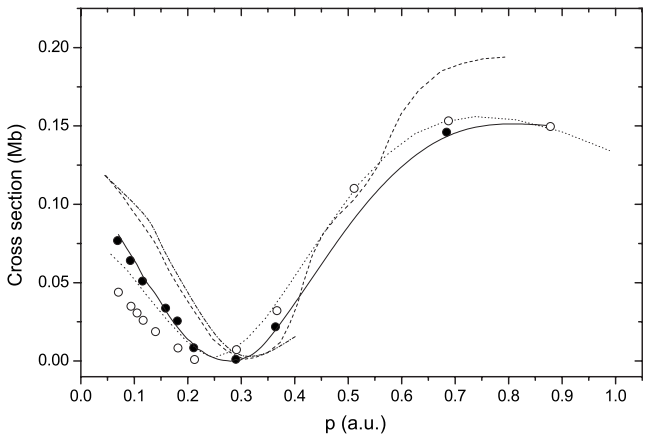


FIG. 2. Comparison of Na photoionization cross sections: dashed-dotted line, best values of Ref. [1]; long dashed line, experiment of Ref. [18]; solid line, current FI3 RMBPT (40/60 splines); solid circles, BO+SR+RPA theory; short dashed line, RRPA calculations of Ref. [5]; open circles, current RRPA 40/60 splines.

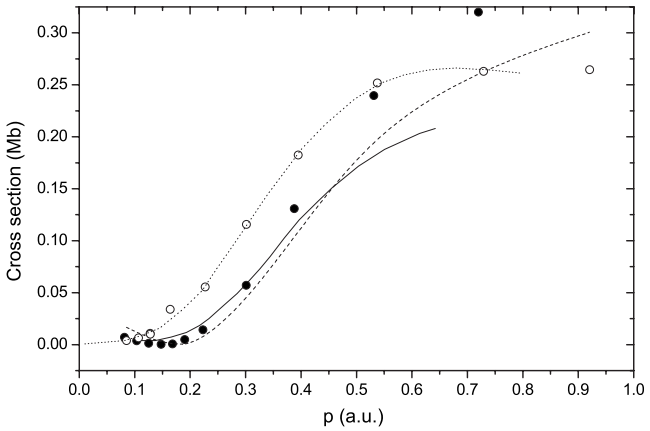


FIG. 3. Comparison of K photoionization cross sections: solid line, experiment, best values from Ref. [1]; short dashed line, RRPA of Ref. [5]; open circles, current RRPA 60 splines; long dashed line, FI3; solid circles, BO+SR+RPA 60 splines.

we discussed in the introduction. It is expected that theory for Na should be more accurate than for heavier alkali-metal atoms, and because good agreement is achieved for K, Rb, and Cs, one can conclude that experiment is less accurate in Na than FI3 and BO+RPA+SR theories.

### B. K photoionization cross section

In Fig. 3 we show comparison for K. The first point to make is that current quasicontinuum RRPA results agree accurately with RRPA calculations of Ref. [5], so the normalization factors are correct. Second, good agreement of FI3 and BO+SR+RPA at $p<0.4$ can be noted. Some disagreement at higher momentum could be attributed to slower convergence of RMBPT due to reduction in energy denominators. We also observe that BO+RPA+SR approximation at low energy is somewhat more accurate than FI3. The superior accuracy of BO+RPA+SR will become more obvious in heavier alkali-metal atoms such as Rb and Cs, considered next. Also we find that significant improvement is achieved compared to previous RRPA calculations of Ref. [5] by including third-order corrections.

### C. Rb photoionization cross section

Similar to the case of K, the current quasicontinuum RRPA calculations are in close agreement with RRPA calculations of Ref. [5] and are not shown here. Moreover RRPA results are in significant disagreement with experiment. However, BO+SR+RPA theory (Fig. 4) gives good agreement with experiment, especially if the experimental cross section is multiplied by a factor of 1.35 which can be appropriate taking into account uncertainty in Rb density used to extract cross sections from photoabsorption. The agreement of FI3 theory is somewhat worse, but still much better than that of RRPA. So the Rb case reveals the importance of all-order BO corrections neglected in FI3 theory. This property can be related to the problem of the phase shift for calculations of which in cases of continuum wave functions

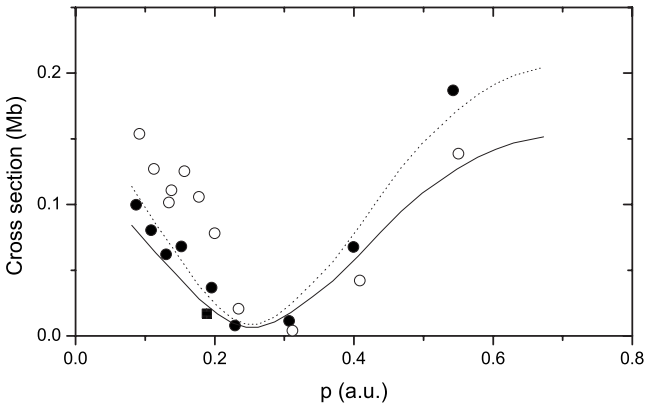


FIG. 4. Comparison of Rb photoionization cross sections: solid line, experiment, best values from Ref. [1]; dashed line, the same experimental data multiplied by 1.35 to account for possible density uncertainty to match better theory; solid circles, BO+SR+RPA (60 splines); open circles, FI3 (60 splines).

of noble-gas atoms BO chain corrections were important [7]. The scatter observed in calculations of FI3 and BO+RPA +SR can be attributed to variations in normalization factors when the cavity sizes and the principal numbers of the quasicontinuum wave functions were varied. Another interesting point is that as photoelectron momentum increases from 0.3 to 0.55 a.u., the divergence between FI3 and BO+RPA +SR monotonously grows, which might be the sign of deterioration of RMBPT accuracy due to the decrease in energy denominators of self-energy. At some point RMBPT will fail to converge and must be replaced with all-order methods such as configuration interaction that allows us to treat core excitation nonperturbatively.

### D. Cs photoionization cross section

Finally, we consider the case of Cs, which has the largest core-polarization effect. In Fig. 5 we compare theoretical calculations performed at different RMBPT approximations. There are several interesting points arising from this comparison. First, one can see large differences between DHF and RRPA, especially at high momentum, meaning large correlation corrections. Second, our quasicontinuum RRPA (open circles) values agree quite well with RRPA results of [5] (dotted line). This, as in cases of other AM atoms, proves fair accuracy of our normalization factors. Moreover, current quasicontinuum DHF values are in close agreement with DHF results of [5] (not shown in Fig. 5). Third, FI3 differs significantly from RRPA, indicating large correlation corrections beyond RRPA. Fourth, FI3 disagrees with BO+RPA +SR theory, and because both contain all third-order terms, the effects beyond third order, in particular BO chaining, are very important in Cs. This is in contrast to the case of Na, where FI3 and BO+RPA+SR theories agreed closely. The BO+RPA+SR theory more or less agrees with BO+RPA calculations of Ref. [6], although in that work only third-order BO correction was included. The calculations of Ref. [6] were in good agreement with experiments normalized at threshold by 0.1 Mb. This threshold is consistent with cross-

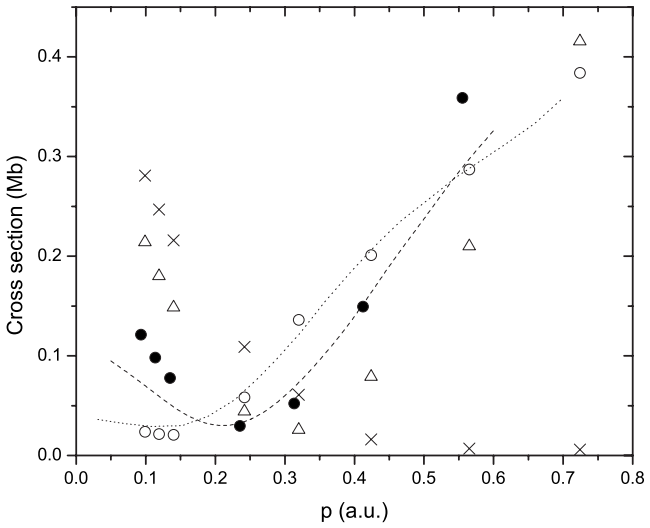


FIG. 5. Comparison for Cs theoretical photoionization cross sections. Current quasicontinuum 60-spline calculations: crosses, length DHF; triangles, length FI3; open circles, length RRPA; solid circles, velocity BO+RPA+SR. Dotted line, continuum RRPA from Ref. [5]; dashed line, continuum BO+RPA from Ref. [6].

section measurements that did not rely on the saturation density equation but used hot-wire measurements to determine the density experimentally [3].

In Fig. 6 we also present a comparison of the best current theory (BO+RPA+SR) with experiment and the theory of Ref. [6]. Since experimental cross sections have uncertainty due to AM density inaccuracy, we have rescaled the experimental values to the best agreement with theory within reasonable range. This scaling factor is not necessarily the best, and several works [2,6] adopted 1.7 smaller normalization,

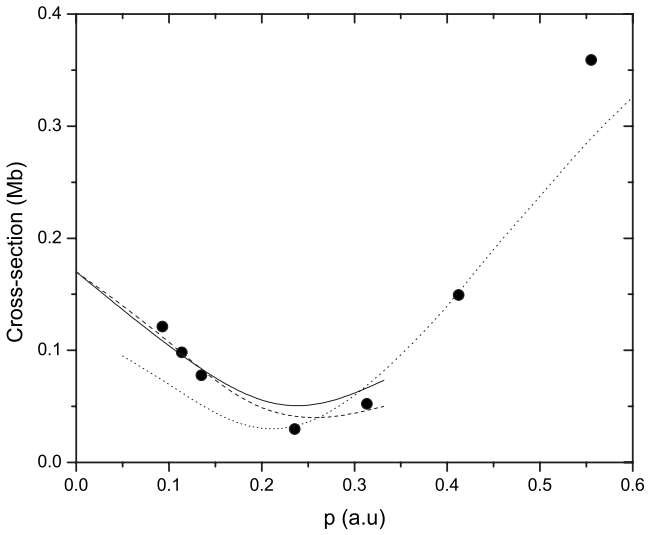


FIG. 6. Comparison of theoretical and experimental photoionization cross sections for Cs. Experimental results of Ref. [1] (solid line) and relative measurement of Ref. [2] are rescaled to the same value at threshold minimum, 0.17 Mb, for best matching our theory. BO+RPA+SR calculations (circles) are compared with experiments and BO+RPA calculations of Ref. [6].

TABLE I. Breakdown of contributions to reduced dipole matrix element for Cs transitions from the ground state to $13p_{1/2}$ and $13p_{3/2}$ quasicontinuum states in the cavity $R=100$ a.u.

| Term | $L\ (p_{3/2})$ | $V(p_{3/2})$ | $L(p_{1/2})$ | $V(p_{1/2})$ |
|---|---|---|---|---|
| DHF | −0.104 | −0.068 | 0.034 | 0.012 |
| RRPA | −0.021 | −0.021 | −0.023 | −0.023 |
| Norm | 0.000 | 0.000 | 0.000 | 0.000 |
| BO3(dressed) | −0.047 | −0.065 | 0.027 | 0.035 |
| SR(dressed) | −0.013 | −0.008 | 0.009 | 0.005 |
| deriv(DHF) | −0.013 | 0.000 | 0.004 | 0.000 |
| Total FI3 | −0.094 | −0.094 | 0.017 | 0.018 |
| RRPA+BO3(dressed) | −0.068 | −0.086 | 0.004 | 0.013 |

but in the original measurements of Ref. [1] and after adjustment using JANAF tables (the cross sections are given in Ref. [2]) cross sections were obtained closer to our rescaled values shown in Fig. 6. At low momentum there is a difference with the calculations of Ref. [6], which included the RRPA and the third-order BO corrections, but neglected the SR and higher-order BO chain corrections. Although the agreement with rescaled experiment was also achieved for this theory, it is not yet obvious that experimental normalization is 100% accurate.

To understand the difference with calculations of Ref. [6], in Table I we show the breakdown of contributions near threshold ($p=0.0988$ a.u.) where the differences were particularly large. The sum of RRPA and BO3 (RRPA dressed) corrections in the table is expected to approach the RRPA+BO(3) theory of Ref. [6], although there is a difference in higher-order corrections due to RRPA dressing. The current RRPA+BO3(RRPA) theory predicts the cross section at $p=0.1$ a.u. to be equal to 0.11 Mb, in much closer agreement with calculations of Ref. [6], which might explain the disagreement with the FI3 theory due to SR and derivative corrections. These corrections, ignored in all previous calculations, according to the table are quite large and important and indicate slow convergence of perturbation theory. Thus although our treatment of RMPBT terms is most complete due to poor convergence it is quite possible that our results might be less accurate than those of some other theories in the case of Cs. Similar situation was observed in calculations of ground-state energy of AM atoms in which second-order theory agreed better than third-order theory.

Another interesting point is the form dependence of BO+RPA theory, which does not include SR and the derivative term, in contrast to form independence of FI3 and RRPA. The form dependence is the ambiguity of theory, unless there is a clear reason for choosing the appropriate form. We also note that the BO correction dominates in third order, meaning that BO chain corrections must be considered, which is done by using BO+RPA+SR theory.

## IV. CONCLUSION

Using quasicontinuum *B*-spline states, photoionization cross sections for Na, K, Rb, and Cs from the ground state are calculated with RMBPT. Current *ab initio* calculations are most complete in terms of inclusion of RMBPT corrections. The improvement in accuracy compared to RRPA is demonstrated for all alkali-metal atoms, although some disagreement with experiment was also observed which could be due to inaccuracy of experiments. This work is the extension of a previous application of RMBPT and quasicontinuum states to the elastic scattering problem. There is a significant potential in this approach because complicated RMBPT codes developed for discrete states do not need modification and all previous work can be leveraged to various continuum problems. This paper illustrates in particular how third-order RMBPT codes can be used for calculations of photoionization cross sections, and this allowed detailed analysis of various perturbation terms. Unfortunately the lack of high-quality experimental data does not allow us to test high-order RMBPT theories of photoionization cross sections at the appropriate level. For such tests it would be necessary to conduct precise experiments in which systematic effects due to density uncertainty are clearly excluded. For example, the measurement of absorption using transitions that are accurately known can provide accurate knowledge of AM density to exclude the dominant systematic effect due to density uncertainty. On the other hand, as the further development of theory, it can be applied to photoionization cross sections of noble-gas atoms, where density and cross sections are known with better accuracy, and maybe to other calculations. The current theory can be used to extend the photoionization database, for example, to calculate photoionization of ions where RMBPT theory have better convergence, but experiments can be difficult. The photoionization of ions is important for modeling plasmas.

[1] G. V. Marr and D. M. Creek, Proc. R. Soc. London, Ser. A **304**, 233 (1968).
[2] H. Suemitsu and J. A. R. Samson, Phys. Rev. A **28**, 2752 (1983).
[3] T. B. Cook, F. B. Dunning, G. W. Foltz, and R. F. Stebbings, Phys. Rev. A **15**, 1526 (1977).
[4] J. C. Weisheit, Phys. Rev. A **5**, 1621 (1972).
[5] M. G. J. Fink and W. R. Johnson, Phys. Rev. A **34**, 3754 (1986).
[6] W. R. Johnson, Indian J. Phys., B **71**, 263 (1996).
[7] I. M. Savukov, Phys. Rev. Lett. **96**, 073202 (2006).
[8] A. Macías, F. Martín, A. Piera, and M. Yánez, Int. J. Quantum Chem. **33**, 279 (1988).
[9] E. M. Isenberg, S. L. Carter, H. P. Kelly, and S. Salomonson, Phys. Rev. A **32**, 1472 (1985).
[10] M. Yan, H. R. Sadeghpour, and A. Dalgarno, Astrophys. J. **496**, 1044 (1998).
[11] I. M. Savukov and W. R. Johnson, Phys. Rev. A **62**, 052512

(2000).
[12] I. Lindgrem and J. Morrison, *Atomic Many-Body Theory* (Springer-Verlag, Berlin, 1982).
[13] V. A. Dzuba and G. F. Gribakin, Phys. Rev. A **49**, 2483 (1994).
[14] V. A. Dzuba, V. V. Flambaum, P. G. Silvestrov, and O. P. Sushkov, J. Phys. B **20**, 1399 (1987).
[15] S. Blundell, D. Guo, W. Johnson, and J. Sapirstein, At. Data Nucl. Data Tables **37**, 103 (1987).
[16] V. A. Dzuba, V. V. Flambaum, A. Y. Kraftmakher, and O. P. Sushkov, Phys. Lett. A **142**, 373 (1989).
[17] J.-J. Chang and H. P. Kelly, Phys. Rev. A **12**, 92 (1975).
[18] R. D. Hudson, Phys. Rev. **135**, A1212 (1964).